POLITECNICO DI TORINO

Corso di Laurea Magistrale
in Sustainable Nuclear Energy

Nuclear Fission Plant

Exercise 2: Thermal Hydraulics in the Hot Sub-channel of an AP1000 Reactor

Professor
Raffaella TESTONI
Cristina BERTANI

Student
Paolo GUIDI s331322
Lara MASSA s331285
Federico PATI s328987

2023/2024

Chapter 1

Introduction

The AP1000 reactor was designed by Westinghouse based on the AP600 design and has been certified by NRC in December 2011. It belongs to the reactors built with passive safety design: it includes significant changes in plant design and layout. Safety, in the event of an accident, depends on passive safety systems (as their name suggests) and safety systems started up by simple actions such as opening valves, but which are passive in operation.

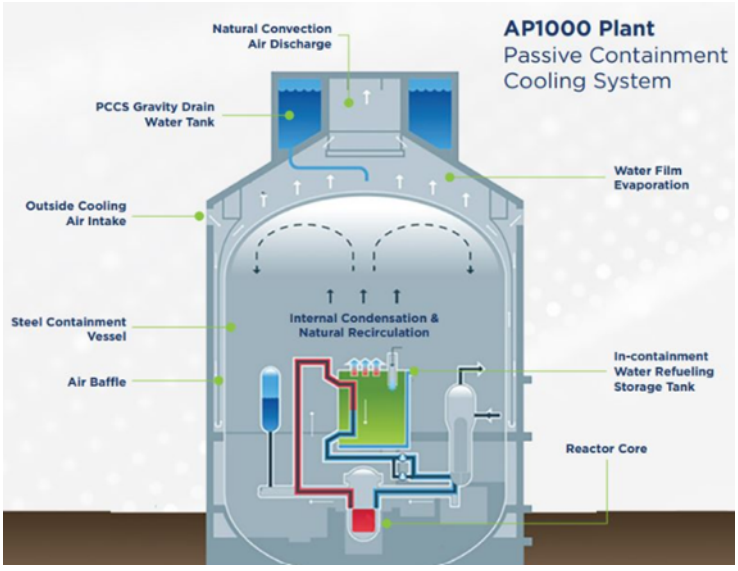

Figure 1.1: The Passive Containment Cooling System of the AP1000 Westinghouse. [1]

The AP1000 is a generation III+ reactor, hence it has additional improvement in safety and it also has undergone improvements from an economic point of view. In fact, the main characteristics of this generation are:

- A standardized design for each type in order to reduce capital cost and reduce construction time;
- A simpler design, that reduces the possibility of failures, makes the reactors easier to operate and less vulnerable to operational upsets;

- Higher availability and longer operating life (typically 60 years);
- Further reduced possibility of core melt accidents;
- Substantial grace period, so that following shutdown the plant requires no active intervention for (typically) 72 hours;
- Resistance to serious damage from an aircraft impact;
- Higher burn-up to use the fuel more fully and efficiently and reduce the amount of waste;
- Greater use of burnable absorbers to extend fuel life.

AP1000 is among the most advanced nuclear reactors, taking advantage of the large experience on PWR designs and operation.

1.1 Mechanical components of the reactor

1.1.1 Fuel grid and rods

The reactor contains a matrix of fuel rods assembled into mechanically identical fuel assemblies along with control and structural elements. The assemblies, containing various fuel enrichments, are configured into the core arrangement located and supported by the reactor internals. The reactor internals also direct the flow of the coolant past the fuel rods.

The fuel grids consist of an egg-crate arrangement of interlocked straps that maintain lateral spacing between the rods. The grid straps have spring fingers and dimples that grip and support the fuel rods. The intermediate mixing vane grids also have coolant mixing vanes. The top, the bottom grids and the protective grid do not contain mixing vanes.

An AP1000 fuel assembly consists of 264 fuel rods in a 17x17 square array. The design is the “17x17 XL Robust” where the fuel assemblies have an active fuel length of 14 feet with no intermediate flow mixing grids.

The fuel rods consist of enriched uranium, in the form of cylindrical pellets of uranium dioxide, contained in ZIRLO™ tubing. The tubing is plugged and seal welded at the ends to encapsulate the fuel. An axial blanket comprised of fuel pellets with reduced enrichment may be placed at each end of the enriched fuel pellet stack to reduce the neutron leakage and to improve fuel utilization.

Fuel rods are pressurized internally with helium during fabrication to reduce clad creep down during operation and thereby prevent clad flattening.

1.1.2 Absorber rods

The rod cluster control assemblies consist of 24 absorber rods fastened at the top end to a common hub, or spider assembly. Each absorber rod consists of an alloy of silver-indium-cadmium, which is clad in stainless steel. The rod cluster control assemblies are used to control relatively rapid changes in reactivity and to control the axial power distribution.

1.1.3 Reactor core

The reactor core is cooled and moderated by light water at a pressure of 2250 psia. Soluble boron in the moderator/coolant serves as a neutron absorber. The concentration of boron is varied to control reactivity changes that occur relatively slowly, including the effects of fuel burnup. Burnable absorbers are also employed in the initial cycle to limit the amount of soluble boron required and thereby maintain the desired negative reactivity coefficients.

The core has inherent stability against diametral and azimuthal power oscillations. Axial power oscillations, which may be induced by load changes, and resultant transient xenon may be suppressed by the use of the rod cluster control assemblies.

Chapter 2

Case Study

2.1 Data

Thermal and Hydraulic Design Parameters	
Reactor core heat output (MWt)	3400
Heat generated in fuel (%)	97.4
System pressure, nominal (MPa)	1.55
Rod pitch (m)	$1.26*10^{-2}$
Coolant	
Effective flow area (m^2)	3.88
Nominal inlet (°C)	279.44
Average rise in core (°C)	81.4
Thermal and Hydraulic Design Parameters	
Heat flux hot channel factor (F_Q)	2.60
Number of fuel assemblies	157
Uranium dioxide rods per assembly	264
Fuel Rods	
Number	41,448
Outside diameter (m)	$9.5*10^{-3}$
Clad thickness (m)	$5.715*10^{-4}$
Fuel Pellets	
Density (% of theoretical)	95.5
Diameter (m)	$8.2*10^{-3}$
Structure Characteristics	
Core height, cold, active fuel (m)	4.267

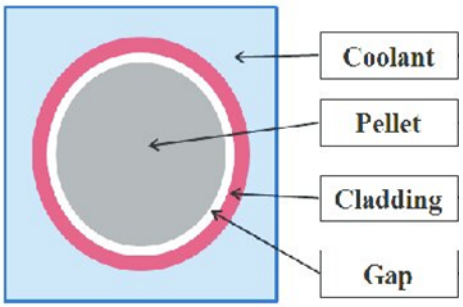

Figure 2.1: Geometrical section of the rod.

2.1.1 Assumptions

It is assumed that the hot channel is closed, and hot-channel factors are considered. The calculation is carried out using the average values of heat flux and flow rate and considering the hot-channel factors evaluated by nuclear calculations.

2.1.2 Objectives

The aim of the exercise is to evaluate the temperature of the coolant, of the cladding and of the fuel at Beginning of Life (BOL) in the hot sub-channel and the minimum value of the DNB Ratio.

Chapter 3

Simulation Setup and Correlations

The first step is the axial discretization of the fuel element and sub-channel considering the active length H on 1000 points. For simplicity the origin (z=0) should be placed in the middle as shown in Figure 3.1 :

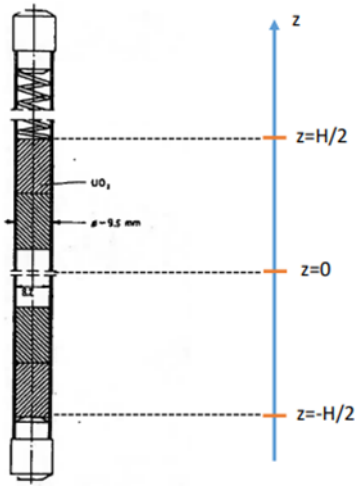

Figure 3.1: Discretization along the length of the fuel element.

3.1 Evaluation of the average volumetric heat generation rate in the core

It is possible to evaluate the average volumetric heat generation rate in the core as follows:

$$q_{v_{ave}} = \frac{P}{V_{fuel}} * 0.974 \tag{3.1}$$

Where:

- $P = 3400 * 10^6\ W$
- $V_{fuel} = N_{rods} * A_{cross_{fuel}} * H_{core}$
- $A_{cross_{fuel}} = \pi * \frac{D^2_{pellet}}{4}$
- The coefficient 0.974 is used to consider that not all the power is generated inside the core, but only the 97.4%.

3.2 Evaluation of the maximum volumetric heat generation rate

Considering the hot-subchannel:

$$q_{v,\max} = q_{v_{ave}} * F_Q \tag{3.2}$$

The distribution of the volumetric heat generation along the length of the fuel can be assumed as:

$$q_{v_{(z)}} = q_{v_{\max}} \cos\left(\frac{\pi z}{H_e}\right) \tag{3.3}$$

The core extrapolated height takes into account the transport mean free path of neutron and the presence of a reflector:

$$H_e = H + 1.42 * \lambda_{tr} + 2 * \delta \tag{3.4}$$

Where:

- Transport length: if the flux is calculated from the diffusion equation, it is assumed to vanish at a small distance d beyond the outer surface of the core.

$$\lambda_{tr} = \frac{1}{\Sigma_{tr}} = 0.29\ cm \tag{3.5}$$

  The parameter d is known as extrapolation distance and for a cylindrical vessel:

$$d = 1.42 * \lambda_{tr} \tag{3.6}$$

- Reflector saving: the neutron reflector scatters back into the core many neutrons that would otherwise escape.

$$\delta = \frac{D_C}{D_R} * L_R \tag{3.7}$$

  - Diffusion coefficient in the core: $D_C = 0.0966\ cm$;
  - Diffusion coefficient in the reactor: $D_R = 0.16\ cm$;
  - Diffusion length in the reflector: $L_R = 2.85\ cm$.

3.3 Evaluation of the average mass velocity in the core

The average mass velocity is the flow rate divided by the flow area:

$$\overline{G} = \frac{\dot{m}}{A_{fl}} \tag{3.8}$$

To evaluate the mass flow rate, it is used the conservation of energy expressed with the enthalpy:

$$\dot{m} = \frac{P}{i_{out_{core}} - i_{in_{core}}} \tag{3.9}$$

The two enthalpies are evaluated with *XSteam* at the nominal pressure of the system and with the two temperatures:

- $T_{in_{core}}$ from the data;
- $T_{out_{core}}$ considering the "Average rise in core" from the data.

For what concern the A_{fl} this have to take care about the bypass contribution and it is taken the "Effective flow area" by the data.

3.4 Evaluation of the coolant specific enthalpy and temperature profiles

The evaluation of the coolant specific enthalpy and temperature profiles is done assuming a chopped cosine distribution as axial power profile.

3.4.1 Specific enthalpy of the coolant

The coolant specific enthalpy profile can be calculated as follows:

$$[i_{(z)} = i_{in} + 1.0267 * \frac{q_v * A_{cross_{fuel}}}{0.974 * W_{HC}} * \left[\sin\left(\frac{\pi * z}{H_e}\right) + \sin\left(\frac{\pi * H}{2 * H_e}\right)\right] \tag{3.10}$$

Where:

- Specific enthalpy at the inlet: i_{in} from the point before;
- Mass flow rate in the hot-channel:

$$W_{HC} = G * A_{width_{cladding}} \tag{3.11}$$

$$A_{width_{cladding}} = \delta^2_{pitch} - \pi * \frac{D^2_{out_{rod}}}{4} \tag{3.12}$$

Two profiles of the enthalpy are calculated:

1. Hot channel enthalpy profile: evaluated with $q_{v_{\max}}$ from (3.2);
2. Average channel enthalpy profile: evaluated with $q_{v_{ave}}$ from (3.1).

3.4.2 Temperature profile of the coolant

Also there two temperature profiles are evaluated, one for the hot channel and the other for the average channel. The temperature profiles are built calculating the difference of temperature between two consecutive points (in 3.13) and adding this value to the last temperature evaluated in (3.15), the value of c_p is an average between the specific heat at the point i and $i+1$, they are evaluated using XSteam whit input data the pressure and the enthalpy.

$$\Delta T_{(i+1)} = \frac{\left|i_{(i)} - i_{(i+1)}\right|}{c_p} \tag{3.13}$$

$$T_{hot\ channel_{(2)}} = T_{in_{coolant}} + \Delta T_{(1)} \tag{3.14}$$

$$T_{hot\ channel_{(i+1)}} = T_{hot\ channel_{(i)}} + \ \Delta T_{(i+1)} \tag{3.15}$$

Obviously for the hot subchannel is used the enthalpy profile of the hot channel and vice versa.

To take in account that in the hot subchannel saturation temperature may be reached, if the temperature calculated is greater than the saturation one, the temperature is fixed to the latter.

3.5 Evaluation of the equilibrim quality profile

The evaluation of the equilibrium quality profile is based on the specific enthalpy, in fact:

$$x_{eq_{(z)}} = \frac{i_{(z)} - i_{ls}}{i_{vs} - i_{ls}} \tag{3.16}$$

i_{ls} is the specific enthalpy of the saturated liquid and i_{vs} the specific enthalpy of the saturated steam, both evaluated with XSteam at the nominal pressure.

3.6 Evaluation of the cladding outer wall temperature

3.6.1 Cladding outer wall temperature

To evaluate the cladding outer wall temperature is necessary to take eventually into account the presence of sub-cooled boiling. In fact, boiling can occur in the hot channel and the heat transfer coefficient is much greater than in single phase convection. So, are calculated two temperature profiles:

1. Single phase convection temperature:
   a. for turbulent flow, correlation similar to the one by Dittus-Boelter can be adopted, with a correcting coefficient C that accounts for the subchannel geometry:

$$Nu_b = C * \left(\frac{G*D_{eq}}{\mu}\right)^{0.8} * \left(\frac{c_p * \mu}{k}\right)^{0.4} \tag{3.17}$$

   For a square array:

$$C = 0.042 * \frac{w}{D_{out_{rod}}} - 0.024$$

   b. The heat transfer coefficient for the single phase can be extract by the Nusselt number as follows:

$$h_{sp} = \frac{Nu_b * k}{D_{eq}} \tag{3.18}$$

$$D_{eq} = \frac{4 * A_{width_{cladding}}}{p_{wet}} \tag{3.19}$$

$$p_{wet} = \pi * D_{out_{rod}} \tag{3.20}$$

   c. Hence, the temperature profile for the single-phase coolant is the following:

$$T_{co_{sp}} = T_{hot\ channel} + \frac{q_{D_{co}}}{h_{sp}} \tag{3.21}$$

$$q_{D_{co}} = q_v * \frac{D^2_{pellet}}{4 * D_{out_{rod}}} \tag{3.22}$$

k, c_p and μ are evaluated for every temperature of the hot subchannel profile and at the nominal pressure of the system.

2. Subcooled boiling temperature:

a good correlation in fully developed boiling is the Jens-Lottes correlation:

$$T_{co_{JL}} = T_{sat} + 25 * q^{0.25}_{D_{co}} * 10^{-6} * \exp\left(-\frac{p}{62}\right) \tag{3.23}$$

These two temperature profiles are compared and when $T_{co_{sp}} > T_{co_{JL}}$ the subcooled boiling begins: the temperature follows $T_{co_{sp}}$ until this point and then follows the profile of $T_{co_{JL}}$.

3.6.2 Flow quality profile

The flow quality is defined as:

$$x = \frac{\dot{m}_v}{\dot{m}_v + \dot{m}_l} \tag{3.24}$$

Before the bubble detachment the flow quality is 0 because $\dot{m}_v = 0$. After the bubble detachment the flow quality can be evaluated with the Bowring-Rouhani model: Bowring showed that the fractional change in bubble volume due to recondensation, averaged over the slightly subcooled region, is small and therefore is negligible with respect to the other heat fluxes.

The heat exchanged at the heated surface by several mechanisms:

- Latent heat of evaporation q_e ;
- Convection caused by bubble agitation q_a;
- Single-phase heat transfer between patches of bubbles q_{sp};
- Recondensation of the bubbles at the wall q_{cond} (negligible).

$$q = q_e + q_a + q_{sp} \tag{3.25}$$

The component that causes the increase of the vapor quality is the evaporative one, so the actual quality in the subcooled region (neglecting the condensation of bubbles in the colder liquid) is:

$$x = \int_{z_D}^{z} \frac{q_e * p_{wet}}{H_{fg} * W} dz = \int_{z_D}^{z} \frac{(q - q_{sp}) * p_{wet}}{H_{fg} * W * (1 + \varepsilon)} dz \tag{3.26}$$

Where:

- Suggested by Rouhani:

$$\varepsilon = \frac{\rho_l}{\rho_{g,sat} * H_{fg}} * (i_{l,sat} - i_l) \tag{3.27}$$

It is imposed that if $i_{l,sat} < i_l$, $\varepsilon = 0$ because $i_l = i_{l,sat}$ at least due to the presence of the fully developed boiling.

The densities are evaluated at the nominal pressure and at the hot channel temperature profile.

- H_{fg} is the enthalpy difference between the gas one and the liquid one. considering fully Developed Boiling at the bubble detachment: $q_{sp} = 0$, if partial boiling is present at the detachment point:

$$q_{sp} = h_{SP_l} * (T_{sat} - T_l) \tag{3.28}$$

3.6.3 Void fraction

The void fraction can be evaluated considering two regions:

1. From the Onset of Nucleate Boiling (ONB) to the bubble Detachment (D): void fraction is zero until the ONB and from there to D it has a linear behaviour and there it can be calculated by Maurer correlation:

$$\alpha = \frac{4 * \delta}{D_h} \tag{3.29}$$

Where:

- The hydraulic diameter:

$$D_h = \frac{p_{wet}}{\pi} \tag{3.30}$$

- For the thickness of the bubble layer the Bowring method can be applied assuming hemispherical bubbles and to cover 50% of the wall surface. These assumptions leads to:

$$\delta = 0.0666 * R_D$$

With the bubble radius at the detachment suggested by Rouhani:

$$R_D = \frac{2.37 * 10^{-3}}{p^{0.237}}$$

2. From the bubble Detachment (D) to the outlet it can be used the correlation with the Slip Ratio:

$$\alpha = \frac{x}{x + (1-x) * \frac{\rho_g}{\rho_l} * S} \tag{3.31}$$

With the Slip Ratio by Fauske, accurate also at not high void fraction:

$$S = \left(\frac{\rho_l}{\rho_g}\right)^{\frac{1}{2}} \tag{3.32}$$

The densities are evaluated at the nominal pressure with *XSteam* for saturated gas and liquid.

3.7 Evaluation of the cladding inner wall temperature

The evaluation of the cladding inner wall temperature must be done considering the dependency of Zircaloy thermal conductivity on the temperature:

$$k_{cl} = 11.45 + 1.425 * 10^{-2}\ T \tag{3.33}$$

The cladding thermal conductivity is evaluated with an average between the T_{co} and the $T_{ci_{guess}}$ of the iteration.

The inner cladding temperature is computed starting from the in the following conductivity integral. Inserting the equation of the cladding thermal conductivity, the integral could be evaluated analytically:

$$\int_{T_{co}}^{T_{ci}} k_{cl} dT = q_v * \frac{A_{cross_{fuel}}}{2\pi} \log(\frac{D_{ci}}{D_{co}}) \tag{3.34}$$

3.8 Evaluation of the temperature on the surface of the fuel pellet

Two guesses are made on the temperatures:

1. On the surface fuel pellet is supposed a difference of 200°C with the internal cladding temperature;
2. On the gap temperature is made an average with the surface fuel pellet temperature guessed and with the internal cladding temperature.

These two calculations are done to evaluate some properties of the materials inside an iteration process until a convergence on the temperatures is found.

3.8.1 Thermal expansion

Uranium dioxide expands more than Zircaloy:

- The pellet diameter changes when the temperature is increased from the ambient temperature:

$$D_{pellet}^{T_a} = D_{pellet}^{T_a} * \alpha_f * \left(\overline{T_f} - T_a\right) \tag{3.35}$$

  Where:

$$\alpha_f = 7.87 * 10^{-6} + 3.9 * 10^{-9} * T \tag{3.36}$$

  Evaluated with the surface fuel temperature guessed.

- The cladding diameter change is:

$$D_{in_{rod}}^{T} - D_{in_{rod}}^{T_a} = D_{in_{rod}}^{T_a} * \alpha_{cl} * \left(\overline{T_{cl}} - T_a\right) \tag{3.37}$$

$$\alpha_{cl} = 5.62 * 10^{-6} + 3.162 * 10^{-9} * T \tag{3.38}$$

  Evaluated with the average temperature on the thickness of the cladding.

3.8.2 Cladding elastic deformation

In an infinite cylinder the radial deformation due to pressure is given by:

$$\Delta D_{in_{rod}} = D_{in_{rod}} * \frac{1}{E} * \frac{1}{\gamma^2 - 1}\left(p_{in}\left[(1-\nu) + (1+\nu) * \gamma^2\right] - 2 * \gamma^2 * p_{out}\right) \tag{3.39}$$

With:

- $\gamma = \frac{D_{out_{rod}}}{D_{in_{rod}}}$ where $D_{in_{rod}}$ is the one calculated just before;
- $\nu = 0.43$;
- $E_{Zr} = 1.148 * 10^{11} - 5.99 * 10^{7} * T$ evaluated at the average temperature on the thickness of the cladding;
- $p_{in} = 35e5 * \frac{T_{gap}}{T_{amb}}$ is assumed to grow linearly with the temperature, starting from 35 bar when the rod is at ambient temperature;
- $p_{out} = 155bar$ the nominal pressure of the system.

3.8.3 Temperature on the surface of the fuel pellet

To evaluate the temperature on the surface of the fuel pellet must be considering the gap conductance:

$$T_{f,S_{(z)}} = T_{ci_{(z)}} + \frac{q_{v_{(z)}} * A_{cross_{fuel}}}{\pi * D_{fuel} * h_g^T} \tag{3.40}$$

Where h_g^T is the total gap conductance that consider the change of pellet and cladding sizes due to thermal field (thermal expansion) and mechanical loads (different pressure between the inner and outer side of the cladding).

The gap conductance is composed by three parallel thermal resistances:

$$h_g^T = h_{rad} + h_{gap} + h_{contact} \tag{3.41}$$

Where:

- Radiative heat transfer coefficient:

$$h_{rad} = \sigma * \frac{T_{f,S}^4 - T_{ci}^4}{T_{f,S} - T_{ci}} * \frac{1}{\frac{1}{\varepsilon_f} + \frac{1}{\varepsilon_{cl}} - 1} \tag{3.42}$$

  ε_f and ε_{cl} can be assumed equal to 1 and evaluated at the surface fuel temperature guessed.

- Gap component can be computed for example with Ross and Stoute correlation:

$$h_{gap} = \frac{k_{gas}}{\beta_2 \left(R_f + R_{Cl}\right) + \delta + l_f + l_{cl}} \tag{3.43}$$

$$\delta = \frac{D_{in_{rod}} - D_{pellet}}{2} \tag{3.44}$$

$$\beta_2 \left(R_f + R_{Cl}\right) + l_f + l_{cl} \approx 2.54 * 10^{-3}\ cm$$

$$k_{gas} = A * T^N \rightarrow A = 0.1763 * 10^{-2}\ and\ N = 0.77163$$

  The latter one is evaluated with the gap temperature guessed.

  The entire loop of iterations built to exit when the relative error is smaller than tolerance of 1e-7.

  From cold to hot conditions, the gap thickness reduces, since the thermal expansion of the fuel is higher than the cladding one.

3.9 Evaluation of the temperature at the centre of the fuel pellet

A guess is done on the temperature at the centre of the fuel, again due to the need of iterations:

$$T_{f,CL_{guess}} = T_{f,S} + 400$$

The evaluation of the temperature at the centre of the fuel pellet is done considering the dependency of UO_2 thermal conductivity on the temperature. From Westinghouse:

$$k_{UO_2} = \frac{1}{11.8 + 0.0238 * T} + 8.775 * 10^{-13} * T^3 \tag{3.45}$$

And the fuel centreline temperature could be deduced solving analytically the conductivity integral, integrating the previous equation of the thermal conductivity:

$$\int_{T_{f,S}}^{T_{f,CL}} k_{UO_2} dT = f \frac{q_{v_{\max}} D_{pellet}^2}{16 k_{UO_2}} \cos\left(\frac{\pi\ z}{H_e}\right) \tag{3.46}$$

Where f (= 0.96) is the Robertson factor is inserted to take into account that in the centre of the fuel the thermal neutron flux decreases, and this prevent to not overestimate the temperature at the pellet centre.

The iteration cycle has a conclusion when the relative error measured on two following iterations on temperature is lower than a tolerance of 1e-7.

3.10 Evaluation of the Critical Heat Flux

The uniform Critical Heat Flux can be calculated by the W-3 correlation:

$$\begin{aligned} q_c = &\{(2.022 - 0.06238 * p) + (0.1722 - 0.01427 * p) \exp\left[(18.177 - 0.5987 * p) x_c\right]\} \\ &* \left[(0.1484 - 1.596 * x_c + 0.1729 * x_c\,|x_c|) 2.326 * G + 3271\right] \\ &* \left[1.157 - 0.869 * x_c\right] * \left[0.2664 + 0.8357 * \exp\left(-124.1 * D_h\right)\right] \\ &* \left[0.8285 + 0.0003413 * (i_{l,\ sat} - i_{in})\right] \end{aligned} \tag{3.47}$$

W-3 was adapted for rod bundle use by multiplying it by F_s (grid spacer factor), which accounts for bundle effects due to the presence of spacer grids:

$$F_S = \left(\frac{p}{225.896}\right)^{0.5} * (1.445 - 0.0371 * L) * \left\{e^{(x+0.2)^2} - 0.73\right\} + K_S * \frac{G}{10^6} * \left(\frac{\alpha}{0.019}\right)^{0.35} \tag{3.48}$$

Where:

- $\alpha = 0.038$;
- Since there are 8 intermediate grids per assembly, the spaces between two of them are 7 and the distance of each one is:

$$L_S = \frac{H}{7} = 0{,}61\ m = 24\ inches$$

With an interpolation between the values for K_S with 20 and 26 inches, $K_S = 0.053$.

To account for 17x17 fuel assembly F_S has to be multiply by 0.88.

Then to consider that the heat flux is non-uniform it is possible to use the Tong factor [2] evaluated with Lin's correlation:

$$F = \frac{C * \int_{L_{ONB}}^{L_{C,NU}} q_{(z')} * e^{-C\left(L_{c,NU} - z'\right)} dz'}{q_{local}\left(1 - e^{-C * L_{C,NU}}\right)} \tag{3.49}$$

An iterative procedure is done to evaluate the non-uniform heat flux:

- Chose a position past the midplane and DNB (z_{DNB}) is assumed to occur at this location:

$$L_{c,NU} = z_{DNB} - z_{ONB}$$

- The quality at the location chosen is taken equal to x_c and C is evaluated:

$$C = 0.15 * \frac{\left(1 - x_{(L_{C,NU})}\right)^{4.31}}{G^{0.478}} \tag{3.50}$$

- The value of x_c is then used to evaluate q_C^{EU} with equation (3.47);
- The value of F is then determined by Lin's correlation (3.49);
- q_C^{NU} is calculated as:

$$q_C^{NU} = \frac{q_C^{EU}}{F} \tag{3.51}$$

- Repeated the process at several other locations.

3.11 Evaluation of the DNBR

The critical heat flux founded for the Not Uniform configuration can be compared with the operating heat flux and it is represented by the Departure from Nucleate Boiling ratio:

$$DNBR = \frac{q_C^{NU}}{q} \tag{3.52}$$

The q utilized is founded in the point 6 of the evaluation of the outer cladding temperature and indicated as $q_{D_{co}}$.

3.12 Verify thermal limits

To verify if the thermal limits are respected is necessary to have the value of MDNBR and evaluate if it is above a certain value. In this case the reactor is operating at normal condition, so it must be true the following state:

$$MDNBR \geq 1.85 \tag{3.53}$$

Chapter 4

Results

The simulation done using Matlab give the following three first results:

Quantity of interest	**Result**
1. Average volumetric heat generation rate $\overline{q_v}$ [W/m^3]	3.55e+08
2. Maximum volumetric heat generation rate $q_{v_{\max}}$ [W/m^3]	9.24e+08
3. Average mass velocity in the core $\overline{G}$ [kg/s/m^2]	3489.99

Table 4.1: Results of the simulation for the point 1, 2 and 3.

It is possible to confront the results with a PWR of 1000 MWe:

Quantity	**AP1000**	**PWR 1000 MWe**
$\overline{q_v}$ [W/m^3]	3.55e+08	3.50e+08
$q_{v_{\max}}$ [W/m^3]	9.24e+08	12.62e+08
$\overline{G}$[kg/s/m^2]	3489.99	3500

Table 4.2: AP1000 vs PWR 1000 MWe

As it is possible to understand from the Table 4.2, this new generation of reactor do not have big difference in terms of power results, but as said in the introduction their novelty lies in the general safety of the reactor.

The volumetric heat generation rate, as expected, has the profile shown in Figure 4.1. The core has a certain extrapolated length and usually the heat flux of this type of reactor follows a chopped cosine profile, as in this case. In the middle, to an higher neutron flux corresponds an higher volumetric heat generation rate. On the other hand, a lower neutron flux at the boundaries corresponds to a lower volumetric heat generation rate.

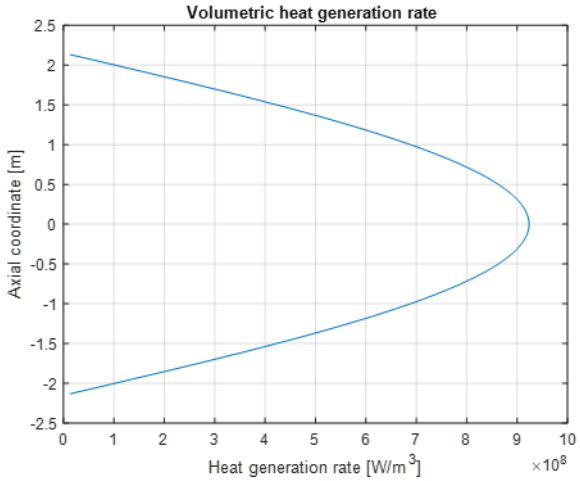

Figure 4.1: Profile of the volumetric heat generation rate

For what concern the coolant specific enthalpy, its profile is reported in Figure 4.2 for the average and the hot channel:

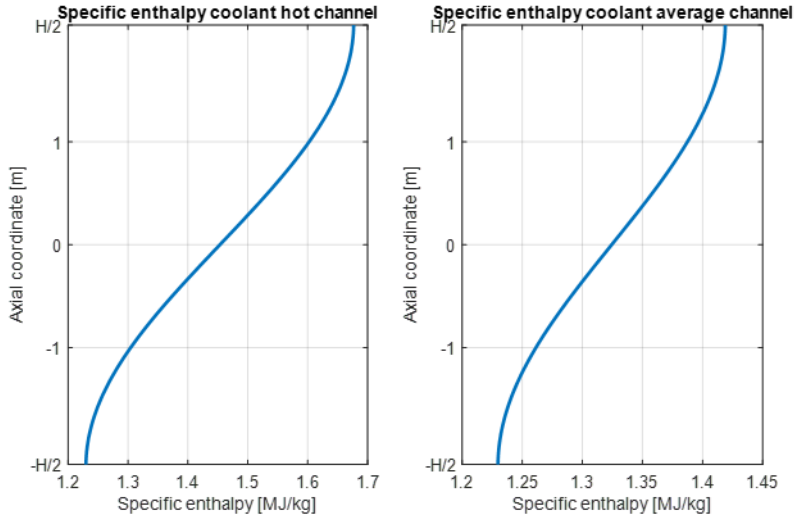

Figure 4.2: Specific coolant enthalpy profiles in the hot and average channels.

The enthalpy rise, as expected, is higher in the hot channel. In fact, this is the coolant channel where the heat flux and enthalpy rise are the largest. Although the reactor is designed to have a heat flux as uniform as possible, there are some areas in which the enthalpy rise is significantly different from the average one, these inhomogeneities appear mainly for physical reasons.

For example, in the centre of the core the neutron flux is higher since the neutron leakages

are lower and this determines a higher number of fissions, or in some areas the coolant flow rate is lower so the enthalpy rise can increase.

There are several strategies to mitigate these phenomena but to collect all of them it is used the hot channel factor:

$$F_{\Delta i} = \frac{\Delta i_{HC}}{\Delta i_C} \tag{4.1}$$

In this case $\overline{F_{\Delta i}} = 2.36$ and it respects the trend: in fact, reactors with a bypass percentage about 9% have a $\overline{F_{\Delta i}} \sim 2$. It is better to have great reduction of the safety factor to have a more uniform power distribution, but the result is expected with the considered bypass mass flow rate.

The coolant temperature profiles follow the enthalpy ones because are directly correlated:

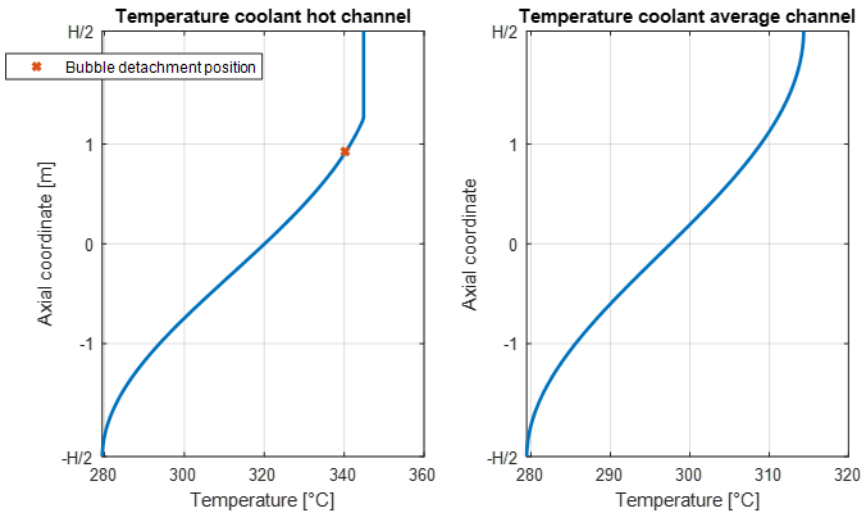

Figure 4.3: Coolant temperature profiles in the hot and average channels

It is possible to see that in the hot channel the saturation temperature is reached above the midplane towards the exit. The bubble detachment is in the subcooled nucleated boiling zone according to the assumption done using the Bowring model.

The equilibrium quality profile is represented in Figure 4.4. It is correctly zero where the hot channel temperature reaches the saturated one and the saturated nucleate boiling zone starts. The slightly sub-cooled region is the region between the bubble detachment position and the axial position where the equilibrium quality reaches zero. It is expected that when the void fraction is calculated, in this range of coordinate, it will increase significantly.

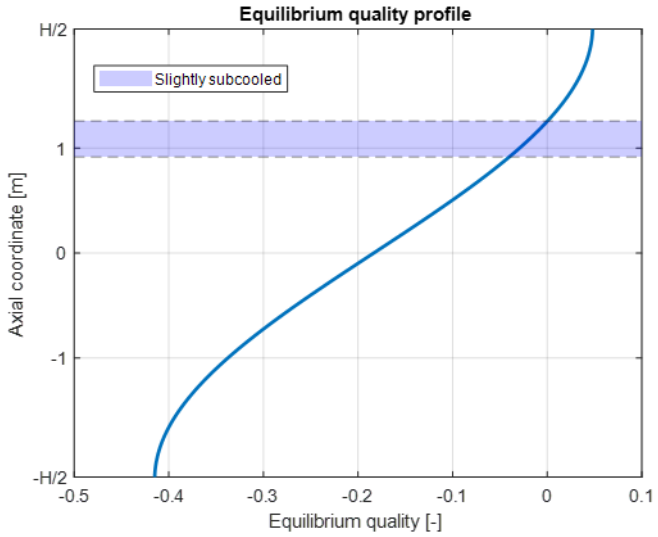

Figure 4.4: Equilibrium quality profile of the coolant.

Moving to the analysis of cladding outer wall temperature, is expected a linear increment in the first part of the profile and almost a constant temperature for the second one.

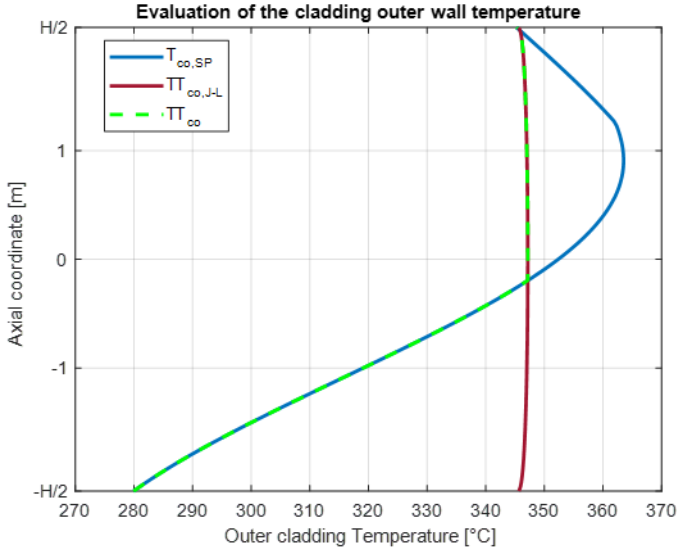

Figure 4.5: Profile of the cladding outer wall temperature.

This is what occurs in the green dashed-line in Figure 4.5. After the first increment, where the outer cladding is cooled by single-phase water, sub-cooled boiling starts and the temperature remains almost constant, following the James-Lottes correlation. This correlation is needed to consider that during the sub-cooled boiling is definitely higher than

in the single phase water. This enhancement allows to have a small temperature difference between the coolant and the cladding even with the high heat flux of the problem.

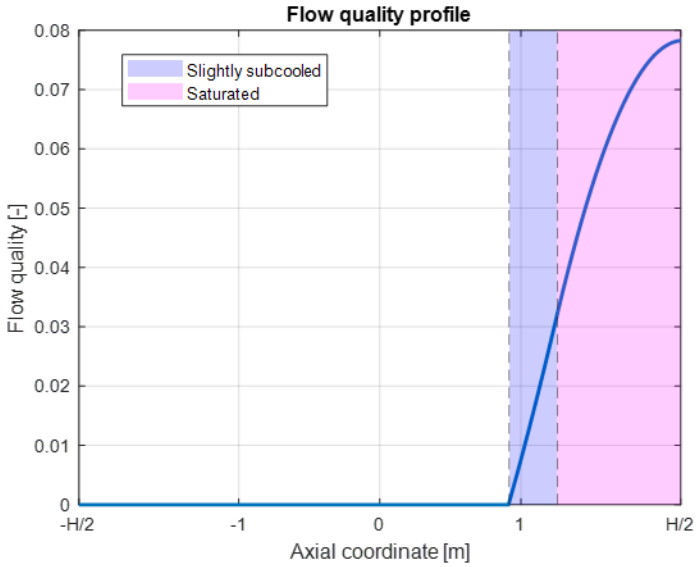

Figure 4.6: Coolant flow quality profile.

This profile corresponds to what was expected since until the point of bubble detachment the bubbles do not detach from the wall, so the flow quality is necessary zero, it then starts to rise firstly in the slightly sub-cooled region then in the saturation region.

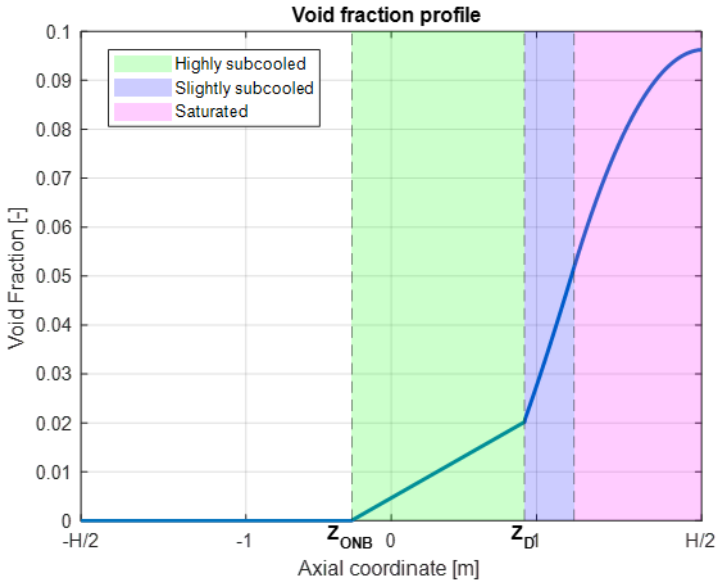

Figure 4.7: Void fraction profile of the coolant

To evaluate the void fraction profile it was used the Maurer correlation (assuming a linear behaviour) in the area between the ONB and the bubble detachment position, after this point it was used the Fauske correlation and as expected the flow quality rapidly increases in the slightly subcooled region. At the exit of the core the void fraction is just under 10%, physically it means that the fraction of area occupied by steam is around 10% of the total one at the exit.

Concerning the temperature in the different radial position:

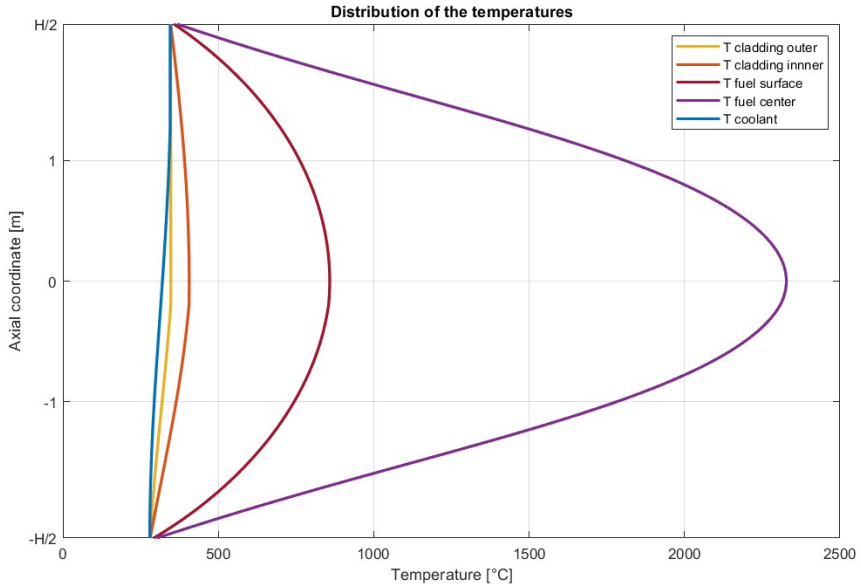

Figure 4.8: Temperature distributions of the fuel and cladding surface.

As expected, temperature in the centerline of the fuel pellet is the highest since the heat deposited by the fissions, even if they occur mainly in the outer part of the pellet, is not very efficiently transferred by the low conductivity of the ceramic UO2 or even removed by a fluid.

	Maximum Temperature [°C]
Fuel surface	858.37
Fuel centerline	2327.52

Table 4.3: Maximum Temperature in the fuel pellet.

Maximum temperature on the centerline and on the surface of the fuel pellet are reported in Table 4.3. Is worth to notice that the fuel temperature is below the uranium dioxide melting point (about 2800°C),so this thermal limit is validated.

The cladding has not a big increase of temperature respect the fuel one because, for example, the gap heat transfer coefficient is lower of about one order of magnitude respect

to the single-phase heat transfer coefficient and $T \propto \frac{1}{h}$: the heat transfer is much lower in the gap respect to the interface with the coolant and this influence a lot the temperatures in the fuel.

The centreline temperature is there calculated with an UO_2 thermal conductivity only influenced by the temperature, it is possible to consider just the UO_2 thermal conductivity since at BOL other factors that can influence the centreline temperature (such as fuel cracking and plutonium content) are not significant, but they will have an important role as the reactor life goes on.

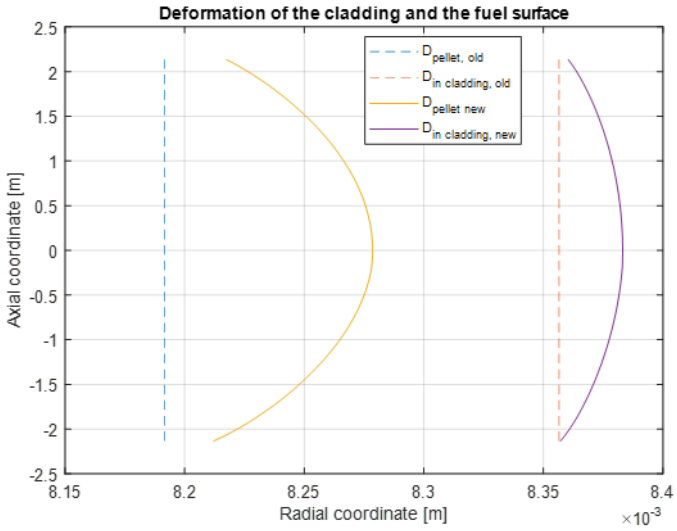

Figure 4.9: Deformation of the cladding and fuel surfaces.

The uranium dioxide expands more than Zircaloy, as visible from the larger increasing of the fuel pellet diameter respect to the inner cladding one.

From the Figure 4.9 it is possible to understand more about the gap between the cladding and the fuel surfaces. It was correct to not consider the contact contribution because the two surfaces do not have contact points and this does not help to rise the gap heat conduction coefficient. In the other hand the other two contributions given by the radiation and the heat exchange in the gap give this contribution:

- Due to the gap: 3497.6 $\frac{W}{m^2K}$
- Due to the radiation: 126.97$\frac{W}{m^2K}$

The largest contribution is given by the heat exchange with the fuel, the cladding and due to the gas, but it is not enough to have a good heat exchange as the coolant interface.

Concerning the critical heat flux in uniform and not uniform conditions the following curves are plotted:

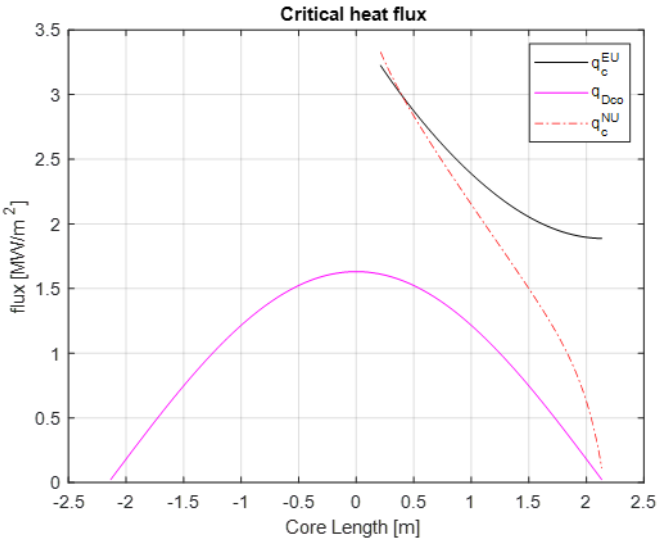

Figure 4.10: Critical heat flux in uniform and not uniform configurations along the core length.

Where $q_{D,co}$ is the heat flux during normal operations and assuming the Departure from Nucleate Boiling (DNB) after the midplane the two critical heat fluxes are evaluated.

q_C^{NU} is calculated only with an experimental factor despite DNB is in the high flux region and is governed primarily by local conditions, but is found that this correction factor can describe in a right way the behaviour of a non-uniform heat flux also from a uniform one. Because of this the Tong factor can be used and it is motivated not only experimentally but also because a "memory factor": the upstream heat flux distributions affect the boundary layer at the DNB position. It is possible to see that the F factor is larger in the outside core length direction, due to a lower q_C^{NU}, this because the memory effect is high the primarily factor that determines the boiling crisis is the average heat flux.

To quantify the thermal margin the distance between the thermal limit (not uniform heat flux, q_C^{NU}) and the operational condition is evaluated: the lower distance in this case is near the exit of the core length. So there the thermal margin is lower, but the thermal limit is respected because the operational condition and the thermal limit do not intersect and so no boiling crisis happens.

Talking about the DNBR and its minimum:

The minimum point of the $DNBR$ is useful to verify that design thermal limits are respected: the larger the ratio is above unity, the lower the risk of boiling crisis. Here the MDNBR is about 1.77 but it does not respect the thermal limit reported on (3.53). It is also possible to observe that MDNBR happens in the subcooled region, in fact $x_{eq} < 0$ and it respect the fact that in the subcooled region, where the value of C is large, the F factor is small the critical heat flux is larger and local heat flux determines the boiling crisis.

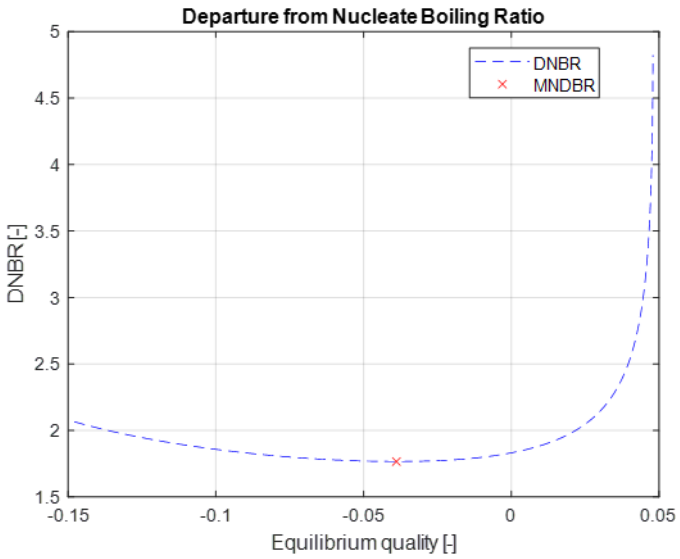

Figure 4.11: DNBR distribution along the equilibrium quality.

Chapter 5

Conclusion

In this report it was analysed the hot channel of a AP1000 under the thermohydraulic aspect, the temperature profiles of different part of the channel were evaluated as well as the quality and void fraction behaviour in the hot channel.

From the analysis of the temperature profile, it appears that in the hot channel the coolant reaches saturation and starts boiling, this can be accepted in a pressurised water reactor since in happens in a low number of sub channel while the average behaviour of the coolant is different since it is far from the saturation point. However, since boiling occurs it is necessary to understand if this causes significant problems to the sub channel, in fact a big presence of vapor can determine both hydrodynamic problems (it increases the friction) and thermal problems (it can significantly reduce the heat exchange between cladding and coolant).

In this case the profile of the cladding and the fuel are always way below the respective melting point, it is important since it means that both the fuel and the cladding do not lose their structural characteristics because of the temperature peak. But studying the DNBR distribution its minimum does not respect the safety standards (in this case it is 1.766 while it must be higher than 1.85). This can be because the flux exiting from the cladding is too high, so to reduce the heat flux through the cladding it can be reduced the volumetric heat generation rate, or it can be varied the gap conductance whit out increasing the fuel temperature at the centre.

Bibliography

[1] URL: https://www.westinghousenuclear.com/energy-systems/ap1000-pwr/overview/.
[2] L S Tong and Joel Weisman. *Thermal analysis of pressurized water reactors*. 3rd ed. La Grange Park, IL: American Nuclear Society, Dec. 1996.

Appendix A

A.1 Exercise 2

```
clear all
close all
clc



%% Dati
power=3400e6; %W
heat_fuel=0.974; % percentuale
psia_to_Pa=6894.76;
pp_nom=psia_to_Pa*2250;

lb_h_ft2_to_kg_s_m2=0.001356;
ft_to_m=0.3048;
pa_to_psi=0.000145038;

number_assembly=157;
fahrenheit_to_celsius=@(T) (T-32)*5/9;
T_in_coolant_core=fahrenheit_to_celsius(535);
T_out_coolant_core=fahrenheit_to_celsius(535+81);
inches=0.0254;
lbm_h_to_kg_s=0.000125998;
ft_2_to_m_2=0.092903;
%% 1
dd_out_rods=0.374*inches;
thickness_cladding_rods=0.0225*inches;
dd_in_rods=dd_out_rods-2*thickness_cladding_rods;
cross_section_rod=dd_out_rods^2*pi/4;

dd_pellet=0.3225*inches;
cross_section_fuel_pellet=pi*dd_pellet^2/4;

HH=168*inches;
```

```
transport_length=0.29e-2;
diffusion_coefficient_core=transport_length/3;
diffusion_coefficient_reflector=0.16;
diffusion_length_reflector=2.85;
reflector_saving=diffusion_coefficient_core*
    diffusion_length_reflector/diffusion_coefficient_reflector;

HH_e=HH+1.42*transport_length+2*reflector_saving;


total_number_rods=41448;
V_fuel=total_number_rods*cross_section_fuel_pellet*HH;

q_v_medio=power*heat_fuel/V_fuel;

%% 2: maximum volumetric heat generation rate
F_Q=2.6; % hot channel factor
q_v_max=q_v_medio*F_Q;

%% 3: Evaluation of the average mass velocity in the core (flow
    rate/flow area): take into account the presence of a bypass
    flow rate.
enthalpy_inlet_core=XSteam('h_pT', pp_nom*1e-5, T_in_coolant_core)
    *1e3;
enthalpy_outlet_core=XSteam('h_pT', pp_nom*1e-5,
    T_out_coolant_core)*1e3;
flow_rate=power/(enthalpy_outlet_core-enthalpy_inlet_core);

factor_bypass=(113.5-106.8)*1e6*lbm_h_to_kg_s/100;
effective_flow_area=41.8*ft_2_to_m_2;
GG=flow_rate/effective_flow_area;
%% 4 Evaluation of the coolant specific enthalpy and temperature
    profiles assuming a chopped cosine distribution as axial power
     profile....
%% Take into account that in the hot subchannel saturation
    temperature may be reached in the hot sub channel.


pitch=0.496*inches;

Ac=pitch^2-(pi*dd_out_rods^2/4);
W_HC=GG*Ac;
ii_z=@(z) (enthalpy_inlet_core + (1.0267*q_v_max*
    cross_section_fuel_pellet*HH_e/(pi*W_HC))*(sin(pi*z/HH_e)+sin(
    pi*HH/(2*HH_e))));

zz=linspace(-HH/2,HH/2,1000);

figure(1)
```

```
enthalpy_distribution_hot=ii_z(zz);
subplot(1,2,1)
plot(enthalpy_distribution_hot/1e6,zz,'LineWidth',2)
ylabel('Axial coordinate [m]')
xlabel('Specific enthalpy [MJ/kg]')
yticks([-HH/2 , -1 , 0 ,1, HH/2]);
yticklabels({'-H/2','-1','0','1', 'H/2'});
ylim([-HH/2,HH/2])
%legend('Coolant',Location='southeast')
title('Specific enthalpy coolant hot channel')

grid on
sat_enthalpy_l=XSteam('hL_p',pp_nom/1e5)*1e3;
T_sat=XSteam('Tsat_p',pp_nom/1e5);

deltaT_hot=zeros(length(enthalpy_distribution_hot)-1,1);

for i= 1:length(deltaT_hot)

    Cp=(XSteam('Cp_ph',pp_nom/1e5,enthalpy_distribution_hot(i)/1e3
    )*1e3+XSteam('Cp_ph',pp_nom/1e5,enthalpy_distribution_hot(i+1)
    /1e3)*1e3)*0.5;
    deltaT_hot(i)=abs(enthalpy_distribution_hot(i)-
    enthalpy_distribution_hot(i+1))/Cp;

end
TT_hot_channel=zeros(length(zz),1);
TT_hot_channel(1)=T_in_coolant_core;
for i =1: length(deltaT_hot)

    TT_hot_channel(i+1)=TT_hot_channel(i)+deltaT_hot(i);
    if TT_hot_channel(i+1)>T_sat
        TT_hot_channel(i+1)=T_sat;
    end
    if isnan(TT_hot_channel(i+1))==true
        TT_hot_channel(i+1)=T_sat;
    end
end
figure(2)
subplot(1,2,1)
plot(TT_hot_channel,zz,'LineWidth',2)
grid on
%legend('Coolant',Location='southeast')
title('Temperature coolant hot channel')

ylabel('Axial coordinate [m]')
xlabel('Temperature [ C ]')
yticks([-HH/2 , -1 , 0 ,1, HH/2]);
yticklabels({'-H/2','-1','0','1', 'H/2'});
```

```
ylim([-HH/2,HH/2])


ii_z=@(z) (enthalpy_inlet_core + (1.0267*1.1*q_v_medio*
    cross_section_fuel_pellet*HH_e/(pi*W_HC))*(sin(pi*z/HH_e)+sin(
    pi*HH/(2*HH_e))));
figure(1)
enthalpy_distribution_average=ii_z(zz);
subplot(1,2,2)
plot(enthalpy_distribution_average/1e6,zz,'LineWidth',2)
grid on
hold on
ylabel('Axial coordinate [m]')
xlabel('Specific enthalpy [MJ/kg]')
yticks([-HH/2 , -1 , 0 ,1, HH/2]);
yticklabels({'-H/2','-1','0','1', 'H/2'});
ylim([-HH/2,HH/2])
%legend('Coolant',Location='southeast')
title('Specific enthalpy coolant average channel')

F_deltai=(enthalpy_distribution_hot(1000)-
    enthalpy_distribution_hot(1))/(enthalpy_distribution_average
    (1000)-enthalpy_distribution_average(1));

sat_enthalpy_l=XSteam('hL_p',pp_nom/1e5)*1e3;
T_sat=XSteam('Tsat_p',pp_nom/1e5);

deltaT_average=zeros(length(enthalpy_distribution_average)-1,1);

for i= 1:length(deltaT_average)

    Cp=(XSteam('Cp_ph',pp_nom/1e5,enthalpy_distribution_average(i)
    /1e3)*1e3+XSteam('Cp_ph',pp_nom/1e5,
    enthalpy_distribution_average(i+1)/1e3)*1e3)*0.5;
    deltaT_average(i)=abs(enthalpy_distribution_average(i)-
    enthalpy_distribution_average(i+1))/Cp;
end
TT_average=zeros(length(TT_hot_channel),1);
TT_average(1)=T_in_coolant_core;
for i =1: length(deltaT_average)

    TT_average(i+1)=TT_average(i)+deltaT_average(i);
    if TT_average(i+1)>T_sat
        TT_average(i+1)=T_sat;
    end
    if isnan(TT_average(i+1))==true
        TT_average(i+1)=T_sat;
    end
end
```

```
figure(2)
subplot(1,2,2)
plot(TT_average,zz,'LineWidth',2)
grid on
yticks([-HH/2 , -1 , 0 ,1, HH/2]);
yticklabels({'-H/2','-1','0','1', 'H/2'});
ylim([-HH/2,HH/2])
ylabel('Axial coordinate')
xlabel('Temperature [ C ]')
title('Temperature coolant average channel')
%legend('Coolant','Location','southeast')
%% 5

enthalpy_sat_steam=XSteam('hV_p',pp_nom/1e5)*1e3;

quality_distribution=zeros(length(TT_hot_channel),1);
for i =1:length(quality_distribution)

        quality_distribution(i)=(enthalpy_distribution_hot(i)-
   sat_enthalpy_l)/(enthalpy_sat_steam-sat_enthalpy_l);

end
figure(3)
plot(quality_distribution,zz,'LineWidth',2)

grid on
xlabel('Equilibrium quality [-]')
ylabel('Axial coordinate [m]')
title('Equilibrium quality profile')
yticks([-HH/2 , -1 , 0 ,1, HH/2]);
yticklabels({'-H/2','-1','0','1', 'H/2'});
ylim([-HH/2,HH/2])

sat_index=1;
while quality_distribution(sat_index)<0 & sat_index<1000
    sat_index=sat_index+1;
    if sat_index==1001
    sat_index=1000;
end

end



%% 6
CC=0.042*pitch/dd_out_rods-0.024;
hh=zeros(1000,1);
p_wet=pi*dd_out_rods;
dd_eq=4*Ac/p_wet;
```

```
209
210 for i=1:length(hh)
211
212 viscosity=XSteam('my_pT',pp_nom/1e5,TT_hot_channel(i));
213 Cp=XSteam('Cp_pT',pp_nom/1e5,TT_hot_channel(i))*1e3;
214 kk=XSteam('tc_pT',pp_nom/1e5,TT_hot_channel(i));
215 if isnan(Cp)==true
216     Cp=XSteam('Cp_pT',pp_nom/1e5,T_sat-0.1)*1e3;
217 end
218
219 if isnan(viscosity)==true
220     viscosity=XSteam('my_pT',pp_nom/1e5,T_sat-0.1);
221 end
222
223 if isnan(kk)==true
224     kk=XSteam('tc_pT',pp_nom/1e5,T_sat-0.1);
225 end
226 Nu_b=CC*(GG*dd_eq/viscosity)^0.8*(Cp*viscosity/kk)^0.4;
227
228 hh(i)=Nu_b*kk/dd_eq;
229 end
230
231
232 q_v_HC=q_v_max*cos(pi*zz/HH_e);
233 q_Dco=q_v_HC*dd_pellet^2/(4*dd_out_rods);
234
235 figure(8)
236 plot(q_v_HC, zz)
237 grid on
238 hold on
239 xlabel('Heat generation rate [W/m^3]')
240 ylabel('Axial coordinate [m]')
241 title('Volumetric heat generation rate')
242
243 TT_co_single_phase=TT_hot_channel'+q_Dco./hh';
244 figure(4)
245 plot(TT_co_single_phase,zz,'LineWidth',2,'Color',"#0072BD")
246 grid on
247 xlabel('Outer cladding Temperature [ C ]')
248 ylabel('Axial coordinate [m]');
249 yticks([-HH/2 , -1 , 0 ,1, HH/2]);
250 yticklabels({'-H/2','-1','0','1', 'H/2'});
251 title('Evaluation of the cladding outer wall temperature')
252
253 TT_co_JL=T_sat+25*(q_Dco*1e-6).^0.25*exp(-pp_nom*1e-5/62);
254 hold on
255 plot(TT_co_JL,zz,'Color',"#A2142F",'LineWidth',2)
256
257 TT_co=zeros(length(TT_co_JL),1);
```

```
a=0;
for i=1:length(TT_co)

    if TT_co_single_phase(i)<=TT_co_JL(i)
        TT_co(i)=TT_co_single_phase(i);
        a=a+1;
    else
        TT_co(i)=TT_co_JL(i);
    end
end

hold on
plot(TT_co,zz,'--','LineWidth',2,'Color',"g")
ylim([-HH/2,HH/2])


%% 6.2

err=1;
toll=1e-10;
detach_index=sat_index;
i=0;
T_detachment_guess=TT_hot_channel(detach_index);
while err>toll
    i=i+1;

    q_detachemnt_guess=q_Dco(detach_index);%hh(detach_index)*(
    TT_co(detach_index)-TT_hot_channel(detach_index)); % andrebbe
    aggiunto il contributo di hNcB vedi slide 'Hot channel heat
    transfer' ma non so come si calcolano tutti i parametri

    hh_detachment_guess=hh(detach_index);

    AAAA=q_detachemnt_guess/(5*hh_detachment_guess);


    T_detachment_new=T_sat-q_detachemnt_guess/(5*
    hh_detachment_guess);


    detach_index=1;
    while TT_hot_channel(detach_index)<T_detachment_new &
    detach_index<1000
        detach_index=detach_index+1;
        if detach_index==1001
            detach_index=1000;
        end
    end
```

```
301     err=abs(T_detachment_new-T_detachment_guess)/
        T_detachment_guess;
302
303     T_detachment_guess=T_detachment_new;
304
305 end
306
307
308
309 figure (4)
310 hold on
311 legend('T_{co,SP}', 'TT_{co,J-L}', 'TT_{co}',Location='best')
312
313 figure(2)
314
315 subplot(1,2,1)
316 hold on
317 plot(T_detachment_guess,zz(detach_index),'x','LineWidth',2.5)
318
319 legend('','Bubble detachment position')
320
321 sat_enthalpy_g=XSteam('hV_p',pp_nom/1e5)*1e3;
322
323 enthalpy_lg=sat_enthalpy_g-sat_enthalpy_l;
324
325 sat_gas_density=XSteam('rhoV_p',pp_nom/1e5);
326
327 figure(3)
328 hold on
329 yline(zz(detach_index), LineStyle="--")
330 hold on
331 yline(zz(sat_index), LineStyle="--")
332 p = patch([-0.5 -0.5 0.1 0.1],[zz(detach_index) zz(sat_index) zz(
        sat_index) zz(detach_index)],'');
333 set(p,'FaceAlpha',0.2)
334 set(p,'EdgeColor','none')
335 %yregion(zz(detach_index),zz(sat_index),"FaceColor", 'v');
336 legend('','','', 'Slightly subcooled')
337 hold on
338
339
340 eps=zeros(length(TT_hot_channel),1);
341 qq=hh'.*(TT_co'-TT_hot_channel);
342
343 qq_primo=q_v_HC*cross_section_fuel_pellet*(zz(end)-zz(end-1))/(pi*
        dd_out_rods*(zz(end)-zz(end-1)));
344 flow_quality=zeros(length(TT_hot_channel),1);
345
346 for i=detach_index:length(TT_hot_channel)
```

```
347     density_liquid=XSteam('rho_pT',pp_nom/1e5,TT_hot_channel(i));
348
349     if isnan(density_liquid)==true
350         density_liquid=XSteam('rhoL_p',pp_nom/1e5);
351     end
352     eps(i)=density_liquid*(sat_enthalpy_l-
    enthalpy_distribution_hot(i))/(sat_gas_density*enthalpy_lg);
353     if eps(i)<0
354         eps(i)=0;
355     end
356
357     q_SP=hh(i)*(T_sat-TT_hot_channel(i));
358     flow_quality(i)=flow_quality(i-1)+(p_wet*(q_Dco(i)-q_SP)*(zz(i
    )-zz(i-1))/(enthalpy_lg*W_HC*(1+eps(i))));
359
360
361 end
362
363 figure(5)
364
365 plot(zz,flow_quality,'LineWidth',2)
366 xlabel('Axial coordinate [m]')
367 ylabel('Flow quality [-]')
368 grid on
369 xticks([-HH/2 , -1 , 0 ,1, HH/2]);
370 xticklabels({'-H/2','-1','0','1', 'H/2'});
371 xlim([-HH/2,HH/2])
372 title('Flow quality profile')
373 hold on
374 xline(zz(detach_index), LineStyle="--")
375 hold on
376 xline(zz(sat_index), LineStyle="--")
377 p= patch([zz(detach_index) zz(detach_index) zz(sat_index) zz(
    sat_index)],[0 0.08 0.08 0],'');
378 q= patch([zz(sat_index) zz(sat_index) zz(1000) zz(1000)],[0 0.08
    0.08 0],'');
379 %p = patch([-0.5 -0.5 0.1 0.1],[zz(detach_index) zz(sat_index) zz(
    sat_index) zz(detach_index)],'');
380 set(p,'FaceAlpha',0.2)
381 set(p,'EdgeColor','none')
382 set(q,'FaceAlpha',0.2, 'FaceColor', 'm')
383 set(q,'EdgeColor','none')
384 legend('','','', 'Slightly subcooled', 'Saturated')
385 hold on
386
387 gas_sat_volume=XSteam('vV_p',pp_nom/1e5);
388 liquid_volume=XSteam('v_pT',pp_nom/1e5,TT_hot_channel(detach_index
    ));
389
```

```
sup_tension=XSteam('st_p',pp_nom/1e5);

liquid_thermal_conductivity=XSteam('tc_pT',pp_nom/1e5,
    TT_hot_channel(detach_index));

T_ONB=sqrt((gas_sat_volume-liquid_volume)*8*sup_tension*T_sat*qq(
    detach_index)/(enthalpy_lg*liquid_thermal_conductivity))+T_sat
    ;

ONB_index=1;

while TT_co(ONB_index)<T_ONB
    ONB_index=ONB_index+1;
end



r_d=2.37e-3/(pp_nom/1e5)^0.237;
thickness_bubble_layer=0.0666*r_d;
%mauer
d_h=p_wet/pi;
void_fraction_d=4*thickness_bubble_layer/d_h;

%void fraction
alpha_zuber=zeros(length(TT_co),1);
alpha_slip_2=alpha_zuber;
alpha_slip_3=alpha_zuber;

delta_alpha=void_fraction_d/(detach_index-ONB_index);

for i=ONB_index:detach_index

    alpha_zuber(i)=delta_alpha+alpha_zuber(i-1);
    alpha_slip_2(i)=delta_alpha+alpha_slip_2(i-1);
    alpha_slip_3(i)=delta_alpha+alpha_slip_3(i-1);
end

%% zuber-findlay
sat_gas_density=XSteam('rhoV_p',pp_nom/1e5);
sat_liquid_density=XSteam('rhoL_p',pp_nom/1e5);

for i=detach_index+1:sat_index-1
    liquid_density=XSteam('rho_pT',pp_nom/1e5,TT_hot_channel(i));
    c0=1.13;
    c1=1.3;
    alpha_zuber(i)=(flow_quality(i)/sat_gas_density)/(c0*(
    flow_quality(i)/sat_gas_density+(1-flow_quality(i))/
    liquid_density)+(c1/GG)*(sup_tension*9.81*(liquid_density-
    sat_gas_density)/liquid_density^2)^0.25);
```

```
433 end
434
435
436
437 for i=sat_index:length(TT_hot_channel)
438     steam_density=XSteam('rho_pT',pp_nom/1e5,TT_hot_channel(i));
439     c0=1.13;
440     c1=1.3;
441     alpha_zuber(i)=(flow_quality(i)/sat_gas_density)/(c0*(
    flow_quality(i)/sat_gas_density+(1-flow_quality(i))/
    sat_liquid_density)+(c1/GG)*(sup_tension*9.81*(
    sat_liquid_density-sat_gas_density)/sat_liquid_density^2)
    ^0.25);
442 end
443
444 %% using slip ratio
445
446 sat_gas_density=XSteam('rhoV_p',pp_nom/1e5);
447 slip_2=(sat_liquid_density/sat_gas_density)^0.5;
448 for i=detach_index+1:sat_index-1
449     liquid_density=XSteam('rho_pT',pp_nom/1e5,TT_hot_channel(i));
450
451     alpha_slip_2(i)=flow_quality(i)/(flow_quality(i)+(1-
    flow_quality(i)*slip_2^-0.5))+void_fraction_d;
452
453
454 end
455
456 sat_liquid_density=XSteam('rhoL_p',pp_nom/1e5);
457 for i=sat_index:length(TT_hot_channel)
458
459    % steam_density=XSteam('rho_pT',pp_nom/1e5,TT_hot(i));
460
461     alpha_slip_2(i)=flow_quality(i)/(flow_quality(i)+(1-
    flow_quality(i)*slip_2^-0.5))+void_fraction_d;
462
463
464 end
465
466 figure(6)
467 plot(zz,alpha_slip_2,LineWidth=2)
468 hold on
469
470
471 x_points = [zz(ONB_index), zz(detach_index)];
472 y_points = [alpha_slip_2(ONB_index),alpha_slip_2(detach_index)];
473 point_text= {'Z_{ONB}', 'Z_D'};
474 % plot L
475 xline(zz(ONB_index), LineStyle="--")
```

```
476 hold on
477 xline(zz(detach_index), LineStyle="--")
478 hold on
479 xline(zz(sat_index), LineStyle="--")
480 hold on
481 t=patch([zz(ONB_index) zz(ONB_index) zz(detach_index) zz(
    detach_index)],[0 0.1 0.1 0],'');
482 p= patch([zz(detach_index) zz(detach_index) zz(sat_index) zz(
    sat_index)],[0 0.1 0.1 0],'');
483 q= patch([zz(sat_index) zz(sat_index) zz(1000) zz(1000)],[0 0.1
    0.1 0],'');
484
485
486 set(t,'FaceAlpha',0.2, 'FaceColor', 'g')
487 set(t,'EdgeColor','none')
488 set(p,'FaceAlpha',0.2)
489 set(p,'EdgeColor','none')
490 set(q,'FaceAlpha',0.2, 'FaceColor', 'm')
491 set(q,'EdgeColor','none')
492 legend('','','', '', 'Highly subcooled','Slightly subcooled', '
    Saturated')
493 hold on
494
495 for k = 1:length(x_points)
496     %plot([x_points(k) x_points(k)], [0 y_points(k)], 'k--');
497     text(x_points(k), 0, sprintf('%s', point_text{k}), '
    VerticalAlignment','top', 'HorizontalAlignment','center',  '
    FontWeight', 'bold');
498 end
499
500 xlabel('Axial coordinate [m]')
501 ylabel('Void Fraction [-]')
502 grid on
503 xticks([-HH/2 , -1 , 0 ,1, HH/2]);
504 xticklabels({'-H/2','-1','0','1', 'H/2'});
505 xlim([-HH/2,HH/2])
506 title('Void fraction profile')
507
508 %% 7
509 kk_cl_funz=@(T)(11.45+1.425e-2*T);
510 TT_ci_guess=TT_co+20;
511
512 err=1;
513 toll=1e-8;
514 i=0;
515 q_Dci=q_v_HC*cross_section_fuel_pellet/(pi*dd_in_rods);
516
517 q_L =q_v_HC*cross_section_fuel_pellet/(pi*2);
```

```
TT_ci_funz = @(T)(11.45.*TT_co+1.425/200.*TT_co.^2-11.45.*T -
    1.425/200.*T.^2 +q_L'*log(dd_out_rods/dd_in_rods))
while err>toll
    i=i+1;
   % kk_cl=kk_cl_funz((TT_co+TT_ci_guess)*0.5);
    %TT_ci=TT_co+(q_Dci'*dd_in_rods./(kk_cl*2)*log(dd_out_rods/
    dd_in_rods));
    TT_ci = fsolve(TT_ci_funz,TT_ci_guess);
    err=norm(TT_ci-TT_ci_guess)/norm(TT_ci-300);
    TT_ci_guess=TT_ci;
end

figure(7)


plot(TT_co,zz, 'LineWidth',2,'Color',"#EDB120")
hold on
plot(TT_ci,zz,'LineWidth',2,'Color',"#D95319")
grid on
xlabel('Temperature [ C ]')
ylabel('Axial coordinate [m]')
yticks([-HH/2 , -1 , 0 ,1, HH/2]);
yticklabels({'-H/2','-1','0','1', 'H/2'});
ylim([-HH/2,HH/2])
%% 8 fuel pellet surface con dipendenza da T

kk_He_funz=@(T)(0.1763e-2*(T+273.15).^0.77163);
TT_fuel_guess=TT_ci_guess+200;
sigma=5.67e-8;
TT_cladding_ave=(TT_ci+TT_co)/2;
TT_gap_ave=(TT_ci+TT_fuel_guess)*0.5;
err=1;
toll=1e-7;

delta=(dd_in_rods-dd_pellet)/2;


T_amb=20;
alpha_cl_funz=@(T)(5.62e-6+3.162e-9*T);
alpha_fuel_funz=@(T)(7.87e-6+3.9e-9*T);
E_zr_funz=@(T)(1.148e11-5.99e7*(T+273.15));

while err>toll

    kk_He=kk_He_funz(TT_gap_ave);
    E_zr=E_zr_funz(TT_cladding_ave);
    alpha_cl=alpha_cl_funz(TT_cladding_ave);
    dd_cl_T=dd_in_rods*(1+alpha_cl.*(TT_ci-T_amb));
    gamma=dd_out_rods./dd_cl_T;
```

```
565     p_in=35e5*((TT_gap_ave+273)/(T_amb+273)); % CONTROLLARE
566     v_poisson=0.43;
567     delta_dd_ci=dd_in_rods*((p_in.*((1-v_poisson)+(1+v_poisson).*
    gamma.^2)-2.*gamma.^2.*pp_nom))./(E_zr.*(gamma.^2-1));
568
569
570     TT_gap_ave=(TT_fuel_guess+TT_ci)/2;
571
572     alpha_fuel=alpha_fuel_funz(TT_fuel_guess);
573     dd_fuel_T=dd_pellet*(1+alpha_fuel.*(TT_fuel_guess-T_amb));
574
575     dd_cl_T=dd_in_rods*(1+alpha_cl.*(TT_gap_ave-T_amb));
576     dd_cl_T=dd_cl_T+delta_dd_ci;
577     delta=(dd_cl_T-dd_fuel_T)/2;
578
579
580     h_gap=kk_He./(2.54e-5+delta);
581
582     h_rad=sigma*((TT_fuel_guess+273.15).^4-(TT_ci+273.15).^4)./((
    TT_fuel_guess+273.15)-(TT_ci+273.15));
583
584     h_gT=h_rad+h_gap;
585
586     TT_fuel_new=TT_ci+(q_v_HC'*cross_section_fuel_pellet)./(pi*
    dd_pellet*h_gT);
587
588     err=norm(TT_fuel_new-TT_fuel_guess)./norm(TT_fuel_new-20);
589
590     TT_fuel_guess=TT_fuel_new;
591     TT_gap_ave=(TT_ci+TT_fuel_guess)*0.5;
592
593
594 end
595 hold on
596  plot(TT_fuel_new,zz,'LineWidth',2,'Color', "#A2142F")
597
598
599 %% 9
600 k_UO2_funz=@(T)(1./(11.8+0.0238*T)+8.775e-13*T.^3)*100;
601 TT_fuel_center_guess=TT_fuel_new+400;
602
603 k_UO2=k_UO2_funz((TT_fuel_center_guess+TT_fuel_new)*0.5);
604  k_UO2_ave=mean(k_UO2);
605 rob_factor=0.96;
606
607 err=1;
608 toll=1e-7;
609 i=0;
610 cross_section_fuel = dd_fuel_T.^2/4*pi;
```

```
611 fun_cl = @(TT_fuel_cl)(-500000/119*log(119*TT_fuel_cl+59000)
    +500000/119*log(119*TT_fuel_new+59000)-351/1.6e13*((TT_fuel_cl
    ).^4 - (TT_fuel_new).^4) + rob_factor*q_v_HC'*dd_pellet^2./16)
    ;
612 while err>toll && i<1e4
613     i=i+1;
614     TT_fuel_center_new = fsolve(fun_cl,TT_fuel_center_guess);
615     err=norm(TT_fuel_center_new-TT_fuel_center_guess)/norm(
    TT_fuel_center_guess-300);
616     TT_fuel_center_guess=TT_fuel_center_new;
617 end
618
619
620 max(TT_fuel_center_guess)
621
622 figure(7)
623 hold on
624 plot(TT_fuel_center_new,zz,'LineWidth',2,'Color',"#7E2F8E")
625 hold on
626 plot(TT_hot_channel,zz,'LineWidth',2,'Color',"#0072BD")
627
628 yticks([-HH/2 , -1 , 0 ,1, HH/2]);
629 yticklabels({'-H/2','-1','0','1', 'H/2'});
630 ylim([-HH/2,HH/2])
631
632 legend('T cladding outer','T cladding innner','T fuel surface','T
    fuel center','T coolant')
633 title('Distribution of the temperatures')
634 %% 10
635 Pa_psi=0.000145038;
636 p_psi=pp_nom*Pa_psi;
637 ll_ft=168/12;
638 ks=0.053;
639 G_lb=2.550;
640
641 % chose a location up to ONB
642 DNB_index=550;
643 zz_DNB=zz(DNB_index);
644 zz_ONB=zz(ONB_index);
645 L_C_NU=zz_DNB-zz_ONB;
646
647
648
649 G_ame = 2.55;
650 chf_nu = zeros(length(zz),1);
651 CC=zeros(length(zz),1);
652
653 q_flux = q_v_max.*cos(pi*zz/HH_e).*dd_pellet^2./(4*dd_out_rods);
654
```

```
655 for ii = DNB_index:length(zz)
656
657
658     zz_DNB=zz(ii);
659     NU_index=(DNB_index-ONB_index)+500;
660     L_C_NU=zz_DNB-zz_ONB;
661
662
663     % circa giusto ZZ=linspace(0, L_C_NU, length(1:ii));
664     ZZ=linspace(0, L_C_NU, length(500:ii));
665
666     CC(ii) = 0.15*(1 - quality_distribution(ii))^4.31/(G_ame
    ^0.478)/inches;
667
668
669     integrando=(q_flux(500:ii).*exp(-CC(ii).*(L_C_NU-ZZ)));
670
671     integral_Tong = trapz(ZZ, integrando');
672
673
674     Ftong(ii) = CC(ii)*integral_Tong./(q_flux(ii)*(1 - exp(-CC(ii)
    )*zz(ii)));
675
676     % uniform
677     qc_funz_Lin=(((2.022-0.06238*pp_nom/1e6)+(0.1722-0.01427*
    pp_nom/1e6)*exp((18.177-0.5987*pp_nom/1e6)*
    quality_distribution(ii)))...
678     *((0.1484-1.596*quality_distribution(ii)+0.1729*
    quality_distribution(ii)*abs(quality_distribution(ii)))*2.326*
    GG+3271) * (1.157-0.869*quality_distribution(ii))
    *(0.2664+0.8357*exp(-124.1*dd_eq))*...
679     (0.8285+0.0003413*(sat_enthalpy_l-enthalpy_inlet_core)/1000))
    *1000; % W/m2
680
681
682     fs_funz = ((p_psi/225.896)^0.5*(1.445 - 0.0371*ll_ft)*(exp((
    quality_distribution(ii)+0.2).^2) - 0.73) + ks*G_lb
    *(0.038/0.019)^0.35)*0.88;
683
684     fs(ii)=fs_funz;
685
686     q_uniform(ii) = qc_funz_Lin*fs_funz;
687
688     qnew_NU(ii) = q_uniform(ii)/Ftong(ii);
689     chf_nu(ii) = qnew_NU(ii);
690 end
691
692 figure(10)
```

```
693 plot(zz(DNB_index:end), q_uniform(DNB_index:end)/1e6,'-k','
    DisplayName','q_c^{EU}')
694 xlabel('Core Length [m]')
695 ylabel('flux [MW/m^2]')
696 hold on
697 grid on
698 box on
699 plot(zz,q_Dco/1e6,'-m','DisplayName','q_D_c_o')
700
701
702 plot(zz(DNB_index:end),chf_nu(DNB_index:end)/1e6,'-.r','
    DisplayName','q_c^{NU}')
703 legend
704 title('Critical heat flux')
705
706 %% 11
707
708 DNBR = chf_nu(DNB_index:end)./(q_Dco(DNB_index:end)');
709 [MNDBR,index] = min(DNBR);
710 figure(11)
711 plot(quality_distribution(DNB_index:end),DNBR,'--b','DisplayName',
    'DNBR')
712 hold on
713 grid on
714 plot(quality_distribution(index+DNB_index-1),MNDBR,'xr','
    DisplayName','MNDBR')
715 xlabel('Equilibrium quality [-]')
716 ylabel('DNBR [-]')
717 legend
718 title('Departure from Nucleate Boiling Ratio')
719
720
721
722 massimi=[
723 max(TT_hot_channel)
724 max(TT_co)
725 max(TT_ci)
726 max(TT_fuel_new)
727 max(TT_fuel_center_new)];
728
729
730 %%
731 figure(9)
732 plot(dd_pellet*ones(length(zz),1), zz, LineStyle="--")
733 hold on
734 plot(dd_in_rods*ones(length(zz),1), zz, LineStyle="--")
735 hold on
736
737 plot(dd_fuel_T, zz, LineStyle="-")
```

```
738 hold on
739 plot(dd_cl_T, zz, LineStyle="-")
740 hold on
741 xlabel('Radial coordinate [m]')
742 ylabel('Axial coordinate [m]')
743 grid on
744 legend('D_{pellet, old}', 'D_{in cladding, old}', 'D_{pellet new}'
    , 'D_{in cladding, new}')
745 title('Deformation of the cladding and the fuel surface')
746
747 value_h_rad=sum(h_rad)/length(h_rad);
748 value_h_gap=sum(h_gap)/length(h_gap);
```